

# Integration of 0.1 GHz to 40 GHz RF and Microwave Anechoic Chamber and the Intricacies

Sellakkutti Suganthi\*, Deepal D. Patil, and Elisha Chand

**Abstract**—The aim of this paper is to highlight and elaborate the construction and establishment of a rectangular anechoic chamber (AC) of dimensions  $7\text{ m} \times 4\text{ m} \times 3\text{ m}$  working from 0.1 GHz to 40 GHz. It is an informative checklist giving an insight on the reckoning of chamber dimensions and selection of appropriate absorbers as per the required specifications. It briefs the key features of validation of an anechoic chamber, namely, shielding effectiveness and reflectivity (quiet zone). It describes the intricacies of the integration of systems such as vector network analyzer (VNA), antenna mounting stands, three-axes motorized antenna rotation control circuitry, and customized software. The validation of the established chamber is accomplished for overall shielding effectiveness of  $-80\text{ dB}$  and reflectivity of  $-40\text{ dB}$  in one cubic meter area at the receiving antenna or the antenna under test (AUT) region far away from transmitter say, at 5.5 m separation. This paper covers the measurement results of three broadband horn antennas which can be used as reference antennas for characterization of other antennas in the chosen frequency range. The entire report will certainly be a guideline for any reader or aspirant who is interested in the development of a similar anechoic chamber and looking for complete intricacies.

## 1. INTRODUCTION

Anechoic chambers are a boon, creating an “echo free” zone for antenna testing and measurements. Based on the applications, AC can be classified as anacoustic or a radio frequency (RF) chamber. Hence, construction of an AC is a multi-fold task, involving critical analyses of all the parameters, keeping in mind the place and motive behind the establishment. In view of this, it is important to keep a thorough check on the shielding effectiveness (SE), reflectivity (R) level, and quiet zone (QZ), while minimizing the cost. SE specifies the isolation ability of the AC from the external electromagnetic (EM) interferences whereas the R level indicates the volume in which the EM reflections are converging to a minimum level. Therefore, QZ is that volume of the chamber, where the reflected waves are from the walls, floor, and ceiling, is below a specified minimum level which can be computed by various mathematical modellings. To enhance the QZ performance, some novel polynomial approximations have also been put forth [23, 30, 31].

Generally, rectangular [1], tapered [2], and double-horn [3, 4] AC geometries are majorly discussed and established. However, the ease of construction and lining absorbers on the surface can make rectangular ACs the most appreciated geometry all over the world. Moreover, incorporation of contemporary geometries to construct spherical [5], elliptical [6], and parabolic [7] chambers is changing the face of chambers, one step at a time, by enhancing the quiet zone and reducing absorber usage. With advancement in technology and resources, modeling and analysis of an AC has become more sophisticated, making use of software tools based on the computational electromagnetics (CEM), finite element method (FEM), and finite-difference time-domain (FDTD) methods, or making use of

---

*Received 24 October 2019, Accepted 2 April 2020, Scheduled 13 April 2020*

\* Corresponding author: Sellakkutti Suganthi (drssuga@gmail.com).

The authors are with the RF and Microwave Research Laboratory, ECE Department, School of Engineering and Technology, CHRIST (Deemed to be University), Bangalore, India.

unconventional methods like geometric optics-based systematic solution [24] and approximate image method [27]. In general, an AC consists of three basis layers, in such as metallic, wooden, and absorbing materials.

Initially, sheet metal of various thicknesses is welded onto a metal support skeleton structure. Then, a wooden layer is fitted on the metallic structure, which is coated on one or both sides with distinct grades of galvanized sheet metal. This is a pre-fabrication enclosure. Metals like copper foil or copper screen are fabricated in a similar manner. However, a single shielding system can also be achieved by mounting galvanized metal sheet on plywood. Finally, copper screens can be mounted and spot soldered to wooden studs. Some, or a combination of these sequences, can be adapted for shielding the AC [8]. Welded seam is the most trusted and expensive method for shielding. For this, minimum thickness steel must be field-welded. Also, a continuous metal inert gas welding is made in every seam. All the welds should be ensured to be watertight. The enclosure is independent of the type of construction. A successful design can be implemented by keeping in mind the design for constructability, quality control provisions, welders that are qualified, and well-trained personnel for quality check. Attention must be paid to the following:

- *Floor Shield Design*: The greatest challenge faced during construction is buckling of the floor shield caused by welding heat. The approaches to this have been discussed in [9].
- *Corner Seams*: All corners should be carefully seamed, especially the ones where three surfaces join.
- *In-Process Weld Testing*: To avoid any procedural mistakes and cost of repair, in-process testing is necessary.

The literature presented in [9–12, 32, 34, 35] highlights other innovative methods for building the enclosure and shielding. Grounding of the metallic enclosure must be done to ensure electrical safety, signal control, and security. The importance and mechanism for grounding are discussed in [13] and [14]. In this report, the requirements for the design of a rectangular AC, the materials used, and the integration of the AC with required systems to bring into operation are presented. The performance characterization of three broadband pyramidal horn antennas covering broad frequency ranges such as 0.8 GHz to 18 GHz, 15 GHz to 32 GHz, and 32 GHz to 40 GHz in three slots has been performed. The procedure for the establishment of a full-fledged AC and its validation are briefed along with characterization of reference antennas (RA). The characterization is accomplished by measuring the reflection coefficient ( $S_{11}$ , dB), gain ( $G$ , dB), and  $E$  and  $H$  plane radiation patterns for different frequencies.

## 2. CONSTRUCTION, SCHEMATIC AND ESTABLISHMENT OF THE CHAMBER

Initially, a proposal for designing a rectangular AC of convenient size is planned to cater the needs of the present-day research trends. Accordingly, an AC of length 7 m, breadth 4 m, and height 3 m with the SE of  $-80$  dB,  $R$  level of  $-40$  dB in one cubic meter QZ is decided to be erected so as to utilize the sophisticated instruments like VNA and spectrum analyzer (SA) conveniently. Therefore, a VNA of 9 kHz to 40 GHz and a SA of 1 MHz to 43 GHz (frequency ranges presented in this report are as available in the market) are procured for the said purpose.

In the design and development of AC, the walls of the chamber and different absorbers involved are crucial. The integration of AC with VNA, three-axes motorized antenna mounting stand, personal computer installed with customized software for measurements is the next challenging task. One can also use SA if the received power is to be directly measured. Finally, the characterization and validation of AC is performed through determination of quite-zone and reflectivity levels. The fundamental step is to decide the frequency range of operation, which is from 0.1 GHz to 40 GHz in our case. Many articles and books in [8, 15, 16] deal with the design and construction aspects of ACs. Measurements are made in the far-field, and the range or antenna separation is decided using Eq. (1), where  $r$  is the separation between transmitting and receiving antennas,  $D$  a value corresponding to the largest physical dimension of the antenna used, and  $\lambda$  the operating wavelength.

$$r \geq \frac{2D^2}{\lambda} \quad (1)$$

**Table 1.** Absorber and reflectivity level [Courtesy: Environtech, Ghaziabad].

| Model<br>No.<br>& Shape | Absorber<br>Height<br>(mm) | R level for various frequencies (dB) |            |            |            |            |          |          |          |          |           |           |           |           |
|-------------------------|----------------------------|--------------------------------------|------------|------------|------------|------------|----------|----------|----------|----------|-----------|-----------|-----------|-----------|
|                         |                            | 100<br>MHz                           | 200<br>MHz | 300<br>MHz | 400<br>MHz | 700<br>MHz | 1<br>GHz | 2<br>GHz | 4<br>GHz | 8<br>GHz | 12<br>GHz | 18<br>GHz | 24<br>GHz | 40<br>GHz |
| FC 5,<br>Flat           | 50                         | -15                                  | -16        | -18        | -18        | -18        | -20      | -20      | -20      | -20      | -20       | -20       | -20       | -20       |
| FU 4,<br>Pyramid        | 100                        | -                                    | -          | -          | -          | -20        | -20      | -25      | -38      | -43      | -46       | -50       | -50       | -50       |
| FU 6,<br>Pyramid        | 150                        | -                                    | -          | -          | -          | -21        | -22      | -28      | -39      | -43      | -46       | -50       | -50       | -50       |
| FU 9,<br>Pyramid        | 225                        | -                                    | -          | -          | -23        | -26        | -28      | -32      | -46      | -50      | -50       | -50       | -50       | -50       |
| FU 12,<br>Pyramid       | 300                        | -                                    | -          | -          | -26        | -30        | -40      | -40      | -44      | -50      | -50       | -50       | -50       | -50       |
| FU 18,<br>Pyramid       | 450                        | -                                    | -          | -          | -28        | -33        | -41      | -42      | -48      | -50      | -50       | -50       | -50       | -50       |
| FU 24,<br>Pyramid       | 600                        | -                                    | -          | -          | -30        | -35        | -43      | -44      | -48      | -50      | -50       | -50       | -50       | -50       |
| FU 28,<br>Pyramid       | 650                        | -22                                  | -25        | -27        | -39        | -41        | -47      | -47      | -48      | -50      | -50       | -50       | -50       | -50       |
| FU 30,<br>Pyramid       | 700                        | -23                                  | -26        | -28        | -42        | -44        | -48      | -49      | -50      | -50      | -50       | -50       | -50       | -52       |
| FU 36,<br>Pyramid       | 750                        | -28                                  | -28        | -29        | -50        | -50        | -50      | -52      | -52      | -52      | -52       | -52       | -52       | -52       |

Generally, the chamber size will increase if the frequency is lowered. There should not be much difference between the height and width of the chamber. This is done to bring the reflections from ceiling and floor to the same level. As a rule of thumb, the width and height of the chamber should usually be thrice the diameter of a minimum sphere containing the largest test antenna, so a spacing of minimum  $2\lambda$  should be maintained between the AUT and absorber tips. As per the guidelines in [17, Table 1], the far-field illumination for 0.1 GHz should be  $< 2\lambda$ , that is  $< 6$  m in our case. More precisely, the spacing between the transmitting antenna and AUT is maintained at 5.5 m according to Eq. (1).

A three-layer AC structure consisting of metal sheets, wooden coverage, and finally absorbing materials, is planned to be erected. In our case, the outer wall of the chamber is metallic layer and made up of aluminum frames. In order to provide better insulation from the outer environment, a wooden layer is followed as a second layer. The final absorber layers are glued onto this wooden layer. The door of the AC is a specially made absorber mounted door that is secured by copper beading in order to maintain the measuring environment. Some of the significant absorbers used in our chamber are shown in Fig. 1. The dimensions of the first two layers can be decided as per the outer dimensions of the AC. However, the inner most layer, being absorbing materials, is selected as a foam material coated with a carbon mixture of chemicals (carbon ferrite impregnated polyurethane) so that its absorbing capacity is enhanced over a wide range of frequencies. The processed foam absorbers are fire retardant with zero halogen thereby avoiding formation of toxic gases. The foams are initially cut into flat square and rectangular shapes which act as the base to the tapered pyramidal foams. Since the chamber can be used for both lower frequencies starting from 0.1 GHz and higher frequencies till 40 GHz, the pyramidal absorbers of varying sizes from 50 mm to 610 mm are designed and used. Three wall layers and different foams provide the required SE at various frequencies. The field uniformity (FU) type pyramidal and flat foams and their exhibited SE levels are depicted in Table 1. The dimensions of the selected absorbers used in the construction of the chamber are presented in Table 2.

The metallic door used in the chamber along with its copper beading for tight coupling when the

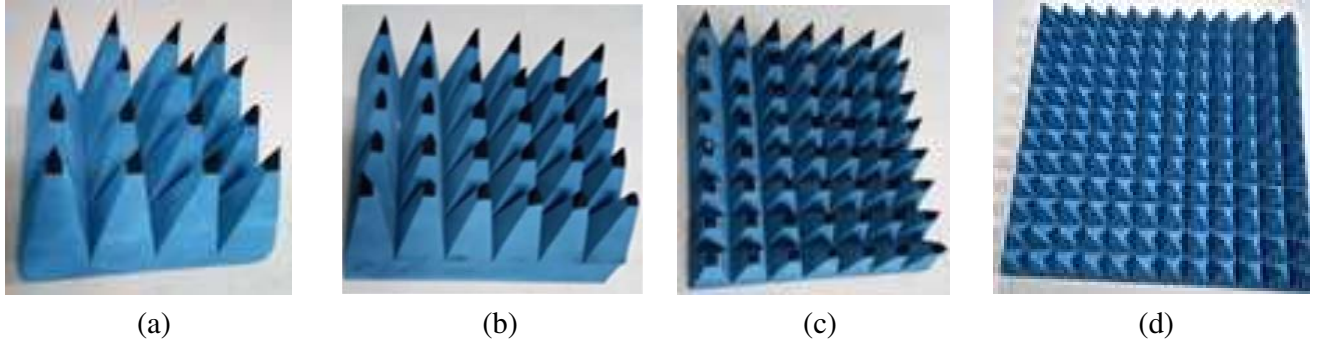


**Figure 1.** Some significant absorbers used in AC, (a) FU 18, (b) FU 12, (c) FU9, (d) FU4.

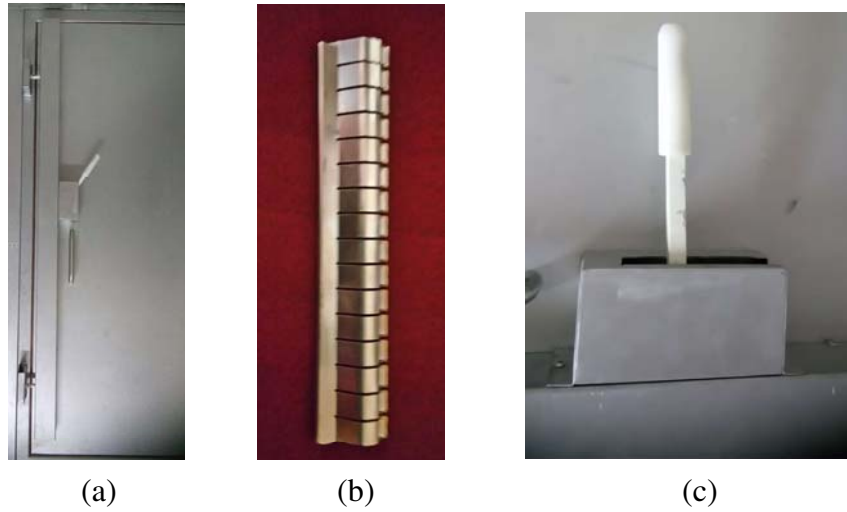


**Figure 2.** Chamber door, (a) metallic wall, (b) copper beading for tight door coupling, (c) door lever.

**Table 2.** Details of absorber dimension [Courtesy: Environtech, Ghaziabad].

| Absorber Model | Placement absorber in chamber                       | Base Height (mm) | Pyramid Height (mm) | Absorber Height (mm) |
|----------------|---|------------------|---------------------|----------------------|
| FU 4           | Transmission wall side                              | 25               | 75                  | 100                  |
| FU 6           | Receiver wall side                                  | 25               | 125                 | 150                  |
| FU 9           | Both side walls. roof & floor                       | 50               | 175                 | 225                  |
| FU 12          | Receiver wall side, both side walls, roof and floor | 100              | 250                 | 350                  |
| FU 18          | Receiver wall side                                  | 75               | 375                 | 450                  |
| FU 24          | Receiver wall side                                  | 100              | 50                  | 610                  |

door remains closed and the type of lever fitted for opening and closing the door are shown in Fig. 2. The physical appearance of the three broadband and high gain horn RAs covering three different frequency ranges are shown in Fig. 3, where the aperture sizes of RA1, RA2, and RA3 are  $28.4\text{ cm} \times 17.2\text{ cm}$ ,  $5.4\text{ cm} \times 3.9\text{ cm}$  and  $3.2\text{ cm} \times 2.5\text{ cm}$  respectively with a uniform metal thickness of 1 mm.

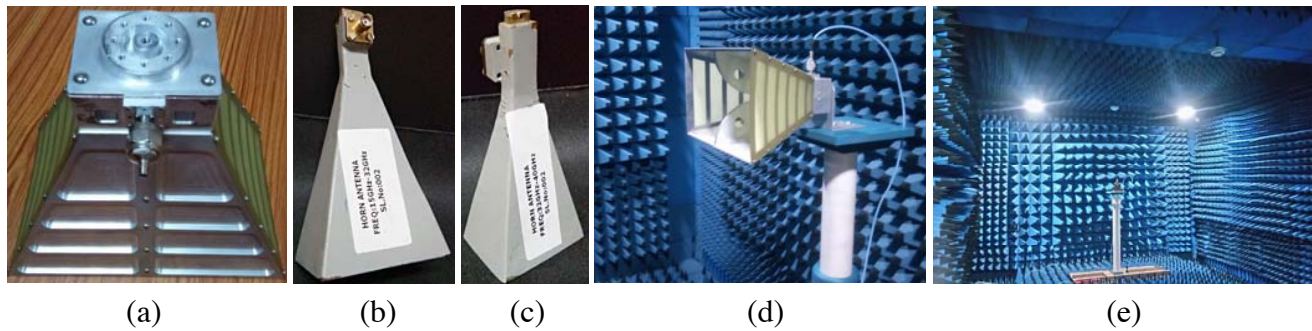


**Figure 3.** Broadband horn reference antennas and stands (a) 0.8 GHz to 18 GHz, (b) 15 GHz to 32 GHz, (c) 32 GHz to 40 GHz, (d) reference transmitting antenna fixed in stand, (e) moving rail type stand used for moving receiving antenna position in quiet-zone measurements.

### 3. COMPLETE SYSTEM INTEGRATION, TESTING AND MEASUREMENT

The constructed AC as described in Section 2 can be validated for specified QZ and SE levels. In order to perform this, integrating the AC and VNA becomes an essential process.

#### 3.1. Integration of Anechoic Chamber and Vector Network Analyzer

The complete system of integration and testing mainly involves the utilization of the following features: AC, fixed transmitter positioner, three-axes receiver positioner with roto-motors, a circuitry to control the three motors, RA (known gain antenna), AUT, testing cables, and control room. A convenient place can be chosen outside the chamber to establish a control room. This can be adjacent to either the transmitting or receiving antenna walls, where the VNA, SA, and personal computer installed with a customized radiation pattern plotting software are placed. The RF and microwave AC provide support in crucial antenna measurements and observations. For making these observations, one needs to study the behavior of  $S$  parameters, which give the fundamental input and output relationship [28] in the antenna measurement. These parameters are fetched by the instrument VNA. Hence it should have a minimum of two ports, and both can be used as input and output ports alternatively as they are reciprocal.

The RA and AUT are connected to the source and receiver ports of the VNA, respectively. Since the AC is to be operated remotely from outside, a customized software has to be developed for feeding the power to RA, controlling the position of AUT, collecting the received power from VNA, and then plotting the desired characteristics. This control circuitry is kept at one corner inside the chamber which is also covered by absorber in order to keep interference to a minimum level. Apart from this, a positioning system is generally needed to hold the antenna in place and to allow the movement in azimuth and elevation angles [22]. In our case, a roto-motor system has a provision for changing the orientation of the antenna in addition to the azimuthal and elevation movements. The schematic of the chamber and control room is shown in Fig. 4.

The input from the VNA is fed to the antenna via a separate RF cable, and the output from AUT is fed to the VNA via another cable. The VNA can be qualified as a versatile device capable of providing data for measuring the resonance characteristics of the AUT and plotting the radiation patterns. These data are fundamental for measuring the return loss, VSWR, impedance, smith chart, radiation patterns ( $E$ -Plane,  $H$ -Plane and 3D polar plots), effective isotropic radiated power, axial ratio, and antenna gain. It is also useful for characterizing filters, power dividers, two port devices, and cables. The screen view of the VNA can be imported as a .png file, and measurement data can be saved as .svna, .csv and .txt formats.

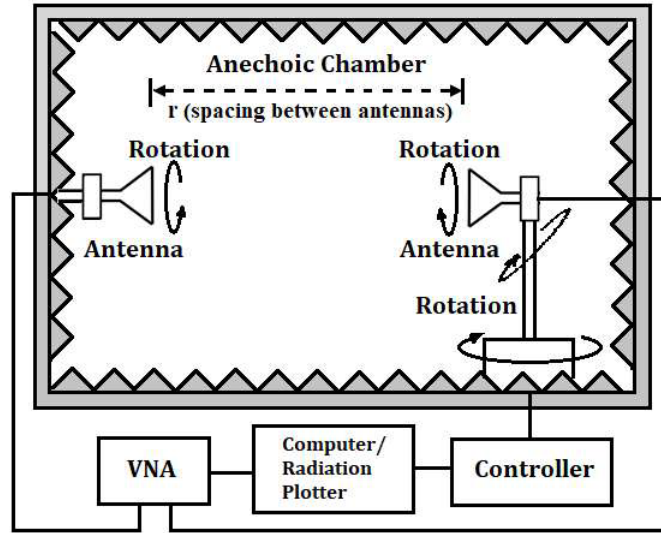


**Figure 4.** Schematic of the anechoic chamber and control room accessories.

### 3.2. Determination of Reflectivity Level and Quiet Zone

The  $R$  level and  $QZ$  are two closely related terms in any anechoic chamber. Conventionally, a free-space voltage standing wave ratio (VSWR) method is used for the measurement of  $R$  level and  $QZ$  [18, 25, 26, 36]. A linear scanning mechanism is generally used to measure the reflectivity. In this method, a probe is moved to scan linearly in the region where the AUT is kept. It is moved up, down, left, and right to observe the different received power levels and to determine finally the  $R$  levels in  $QZ$  volume. Values of these variations are then calculated by measuring the change in field with respect to distance and periodicity. Since this method can cover a limited region in single scan, a manual moving rail system can be used in such a way as to adjust the position of AUT back and forth in the expected  $QZ$  region. However, literature suggests a circular scanning technique where software processing is used to analyze and synthesize the directive response [19] in all the  $360^\circ$  directions. This scanning technique cancels the rear response and maximizes the response in a given direction, which is not possible in the case of linear scanning.

The AUT is mounted on a small flat table, with a manually movable rail type stand kept at the far end of the transmitting antenna. The VSWR measurements are carried out using the VNA. It is assumed that signals in the test region are received by an antenna with isotropic pattern. While using a directional antenna, the differences between the direct signals and reflections are obtained and evaluated [8] to determine the  $R$  level and ultimately the  $QZ$ . Introducing a corner reflector may enhance the absorbing capacity. However, increasing the size of the reflector may further provide higher directivity [20]. The reflectivity performance of the specific absorbers at needed frequency range has to be prepared. A meticulous arrangement of these absorbers inside the chamber will enhance the  $QZ$ . However, in this paper, the arrangement of different absorbers for proving the required  $R$  level and the overall SE is depicted in Fig. 5(a). A view of the control room setup is presented in Fig. 5(b).

It can be noted that the chemically processed foam absorbers used in this chamber are broadband absorbers which are of various sizes and combinations. Even though the foams are designed to absorb normal incidence, grazing incidence and reflections of EM waves from all directions, they exhibit varying SE and  $R$  level at different frequencies as noticed in Table 1. Therefore, the receiver end wall is glued with all kinds of absorbers to provide the maximum possible absorption of EM waves covering all the frequencies of our interest. This is carried out with a view to provide the overall SE of the chamber as  $-80$  dB. However, the average  $R$  level is  $-40$  dB up to 5 GHz in one cubic meter size at the receiver end. It should be noted that the  $QZ$  dimension is not a constant [20] in the entire range of frequencies as the absorbing capacity of the processed foams is a variant. Hence, it changes from one cubic meter



**Figure 5.** Appearance of the full-fledged chamber with all accessories and wall enhanced by different absorbers. (a) Receiver (AUT) and transmitter (reference antenna). (b) Control room with VNA, SA and radiation plotting PC adjacent to AC.

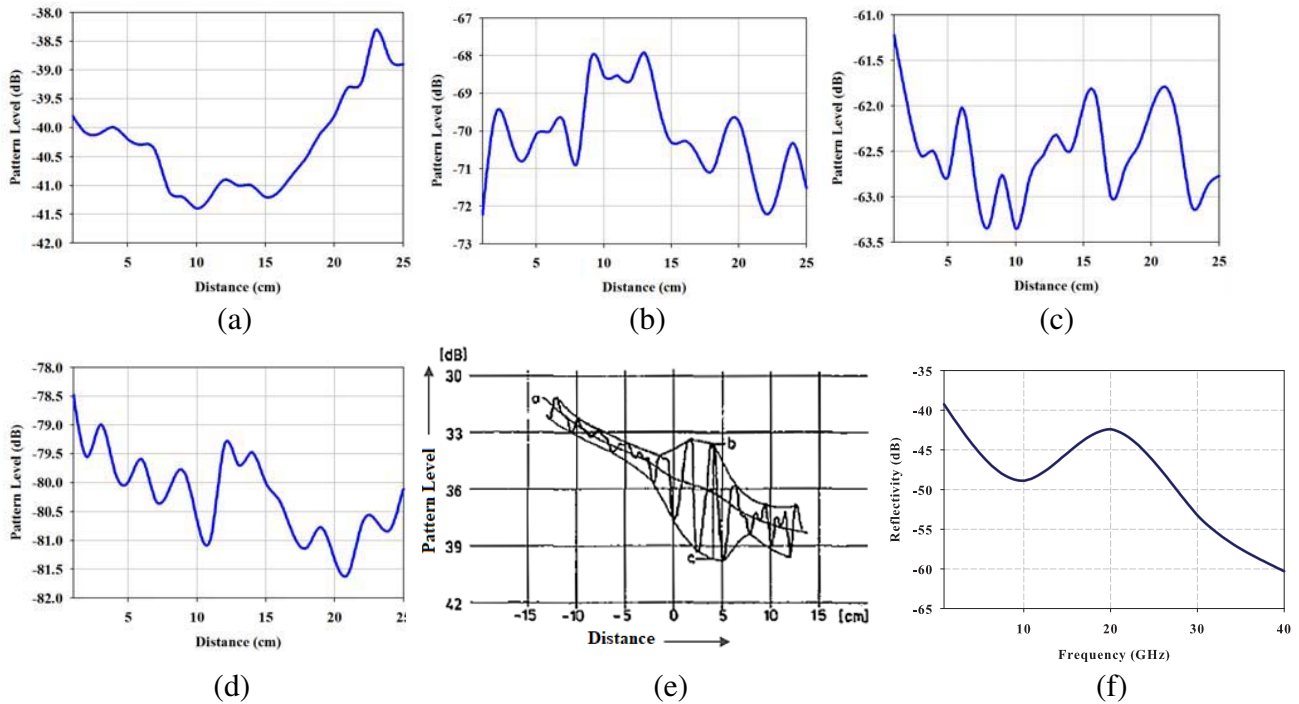


**Figure 6.** Sample pattern level at (a) 800 MHz, (b) 10 GHz, (c) 24 GHz, (d) 40 GHz, (e) sample plot from [8] for comprehension, (f) plot of R level versus frequency for the values presented in Table 3.

to 0.5 cubic meter size at higher frequencies up to 40 GHz.

When two or more identical waves interact with each other, they can either have no effect, can interfere constructively, or can interfere destructively. When the transmitter radiates, the signal at each observed point is a standing wave and is an interference of the intended direct signal and reflected signals. These reflections are the sources of error for the measurements to be made in the AC [8, 36]. Sample measurement results of these interference pattern levels (represented in dB) for some selected frequencies are presented in Figs. 6(a)–(d). These curves depict the interference pattern level between a direct signal, also called the line of sight pattern level ( $L$ , dB) and the reflected signals. For better comprehension, one can consider a similar graph taken from [8] and assume that the obtained standing

**Table 3.** Reflectivity calculations at some sample frequencies.

| Parameters used in<br>reflectivity calculation | Frequency (GHz) |        |        |        |        |         |         |
|--|-----------------|--------|--------|--------|--------|---------|---------|
|  | 0.8             | 4      | 10     | 18     | 24     | 32      | 40      |
| <b>b</b> (dB)                                  | -38.68          | -60.02 | -67.92 | -60.90 | -61.12 | -68.64  | -78.47  |
| <b>c</b> (dB)                                  | -39.00          | -62.67 | -69.32 | -62.40 | -62.50 | -69.72  | -79.50  |
| <b>L</b> (dB)                                  | -34.67          | -36.74 | -41.16 | -43.21 | -35.86 | -37.89  | -44.10  |
| <b>s</b>                                       | 1.0375          | 1.3567 | 1.1748 | 1.1885 | 1.1721 | 1.1324  | 1.1259  |
| <b><math>\rho</math></b>                       | 0.01840         | 0.1513 | 0.0803 | 0.0861 | 0.0792 | 0.06208 | 0.05922 |
| <b>R'</b> (dB)                                 | -34.70          | -16.40 | -21.90 | -21.29 | -22.02 | -24.14  | -24.55  |
| <b>a</b> (dB)                                  | -04.17          | -24.69 | -27.46 | -18.44 | -25.46 | -30.53  | -35.66  |
| <b>R</b> (dB)                                  | -38.87          | -41.09 | -49.36 | -39.44 | -47.48 | -54.67  | -60.21  |

wave is enveloped as shown in Fig. 6(e). In this, the two enveloping curves are drawn loosely and connect all the points of maxima and minima. The point with maximum reflection as observed in the plot is said to be  $b$  (in dB), the corresponding minimum value said to be  $c$  (in dB), and their average pattern level is denoted by  $a$  (in dB). The reflection coefficient  $\rho$  is computed using its relationship with the calculated  $s$  value. The overall reflectivity  $R$  has been computed using these points of maxima and minima through Eq. (2) to Eq. (6) [8, 36, 37]. However, the possibility of the reflections being stronger due to pattern nulls cannot be neglected (that is,  $b < c$ ). This is resolved [36] by considering not one, but the next two to three closest maxima values in the interference curve.

$$s = 10^{\frac{(b-c)}{20}} \quad (2)$$

$$\rho = \frac{s-1}{s+1} \quad (3)$$

$$R' = 20 \log(\rho) = 20 \log\left(\frac{10^{\frac{(b-c)}{20}} - 1}{10^{\frac{(b-c)}{20}} + 1}\right) \quad (4)$$

$$a = \frac{b+c}{2} - L \quad (5)$$

$$R = R' + a \quad (6)$$

In reality, the interference of the direct signal and reflections can be either constructive or destructive. If the interference between direct signal and reflected signal is destructive, next multiple maxima points and their corresponding minima are taken for calculation. This takes care of  $(b-c)$  becoming negative due to  $b < c$ . Table 3 gives a detailed insight to the calculations involved for some sample frequencies. As an example, one set of values obtained for the frequency 800 MHz may be considered for discussion. A reflection coefficient  $\rho$  of 0.0184,  $s$  of 1.0375, and the value  $(b-c)$  of 0.32 dB indicate that a reflection of 1.84/100 of a direct signal produces a ripple level of 0.32 dB which amounts to an actual reflectivity of -34.7 dB and overall reflectivity of -38.87 dB. It is noted that the calculations shown in Table 3 are a set of sample values and by no means denote the entire calculations involved for all the frequencies from 800 MHz to 40 GHz. Hence, the curves appearing in Figs. 6(a)–(d) are a few samples that have been extracted from a large set of measurements made by keeping identical RAs in the AUT side, at the left, right, bottom, front, back, and center points to cover the intended QZ dimensions of one cubic meter. Using the computed values, the overall reflectivity  $R$  is plotted as a function of frequency as depicted in Fig. 6(f).

### 3.3. Determination of Shielding Effectiveness

In general, IEEE 299 and NSA 65-6 are the most common testing procedures used [21, 33] for SE characterization in AC. In these, the enclosure is tested by keeping antennas at appropriate fixed spacing inside the chamber on either side of the enclosure wall. In simpler words, the measurements

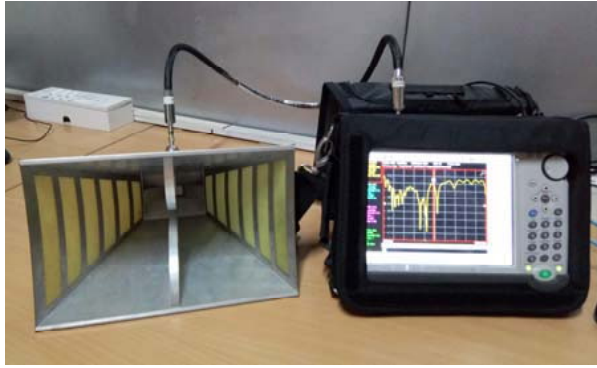


**Figure 7.** VNA as a part of measurement set up.

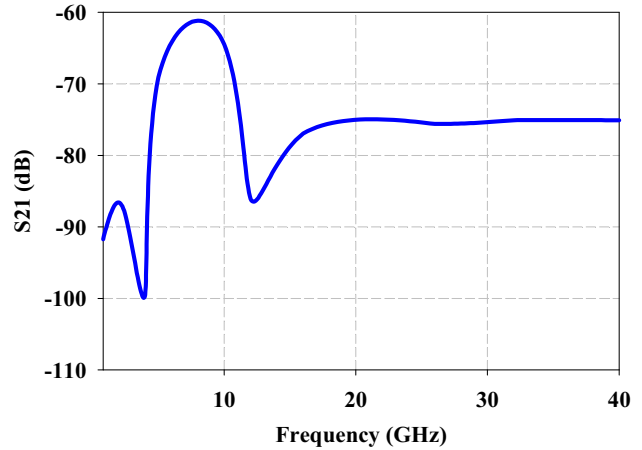


**Figure 8.** Plot of transmitted power inside the chamber for SE computation.

**Table 4.** SE and QZ levels at different frequencies.

| S. No | Frequency (GHz) | QZ (dB) | SE (dB) |
|-------|-----------------|---------|---------|
| 1     | 0.8             | -38.49  | -82     |
| 2     | 4               | -42.26  | -81     |
| 3     | 10              | -58.88  | -82     |
| 4     | 24              | -60.01  | -79     |
| 5     | 40              | -65.48  | -78     |

are made by first keeping the door of the chamber closed and then by leaving it open. The policies and procedures of IEEE standard association categorize the standards as recommended practices, trial-use documents, guides, and standards. All the measurements discussed in this report are done in compliance with IEEE 299/MIL STD 285 [38, 39]. This IEEE Standard 299 is a recommended practice and has proven to be invaluable for decades. The VNA as a part of measurement setup is shown in Fig. 7.

The transmission characteristics can be obtained as a function of frequency when two identical RAs are placed in line of sight inside the chamber. Thus,  $S_{21}$  (dB) characteristics for the three RAs have been plotted together using the measured data obtained from VNA and are shown in Fig. 8. This graph is obtained by using commercial software known as SigmaPlot which takes care of smoothing the curve, and hence the usual small noise over uncorrelated frequency points are not noticeable. In order to compute the overall SE, the average value of  $S_{21}$  (dB) can be taken from the peak value close to -60 dB and the deep value -100 dB. Hence, the performance of the chamber is specified as a single value for the overall SE of -80 dB. Table 4 provides an insight into the varying values of QZ and SE at some selected frequencies. There is a huge set of values as obtained during the testing, and only a selected few are presented in this report for discussion.

### 3.4. Reference Antenna Characterization

As mentioned previously, the frequencies of interest are covered with three customized waveguide antennas. Since the chamber is designed for a large frequency coverage, single antenna providing such a huge bandwidth is practically difficult. Therefore, the performances of these antennas inside the AC were verified by keeping identical RAs as transmitting and receiving antennas. These antennas were initially tested at third party laboratory with antenna separation distance of 6 m and certified. Hence those test results were used as reference, for example, known gain values at various frequencies. The standard Friis transmission formula [29] used to compute the gain characteristics at various frequencies

for the AUT is given by Eq. (7).

$$P_r = P_t G_t G_r \left[ \frac{\lambda}{4\pi r} \right]^2 \tag{7}$$

where  $\lambda$  is the wavelength (in m) corresponding to the operating frequency;  $P_r$  is the received power (in W);  $P_t$  is the transmitted power (in W);  $G_t$  and  $G_r$  are gains (in dB) of transmitting and receiving

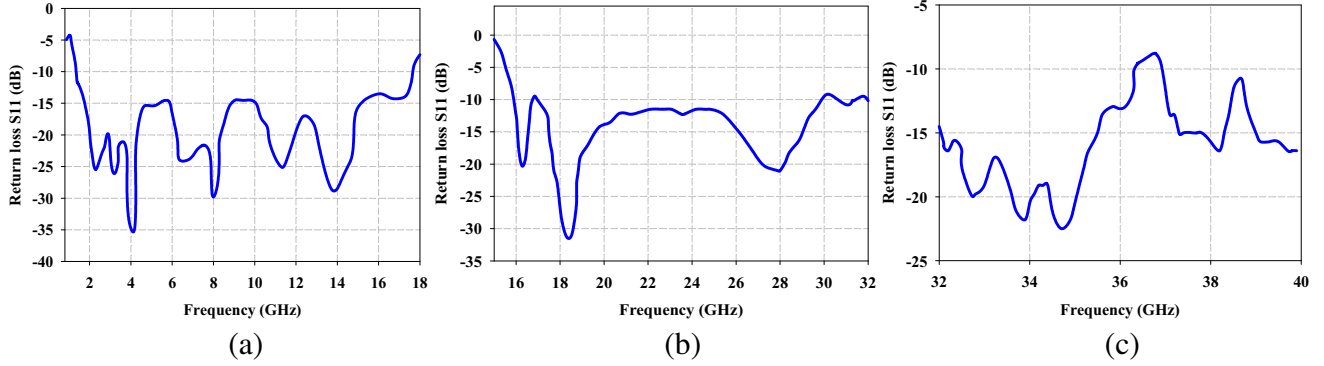


Figure 9. Return loss characteristics, (a) RA1, (b) RA2 and (c) RA3.

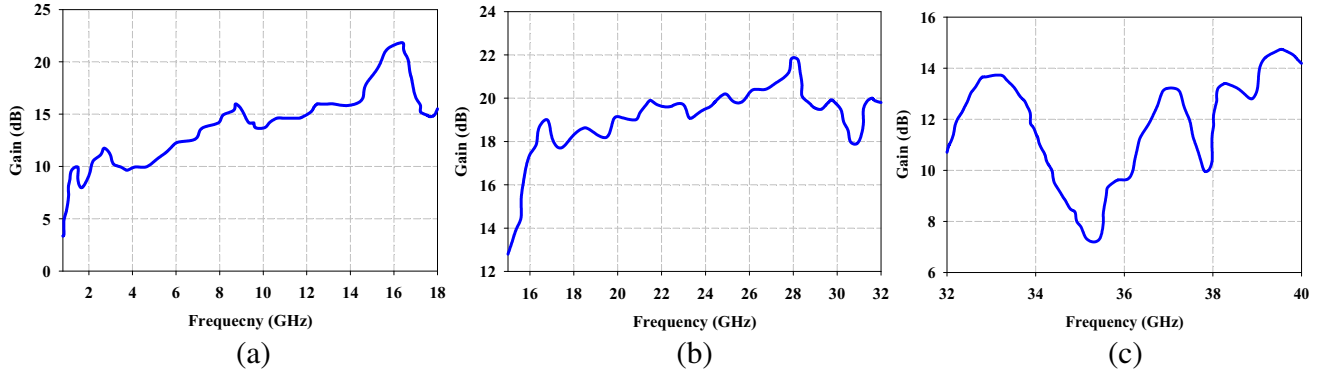
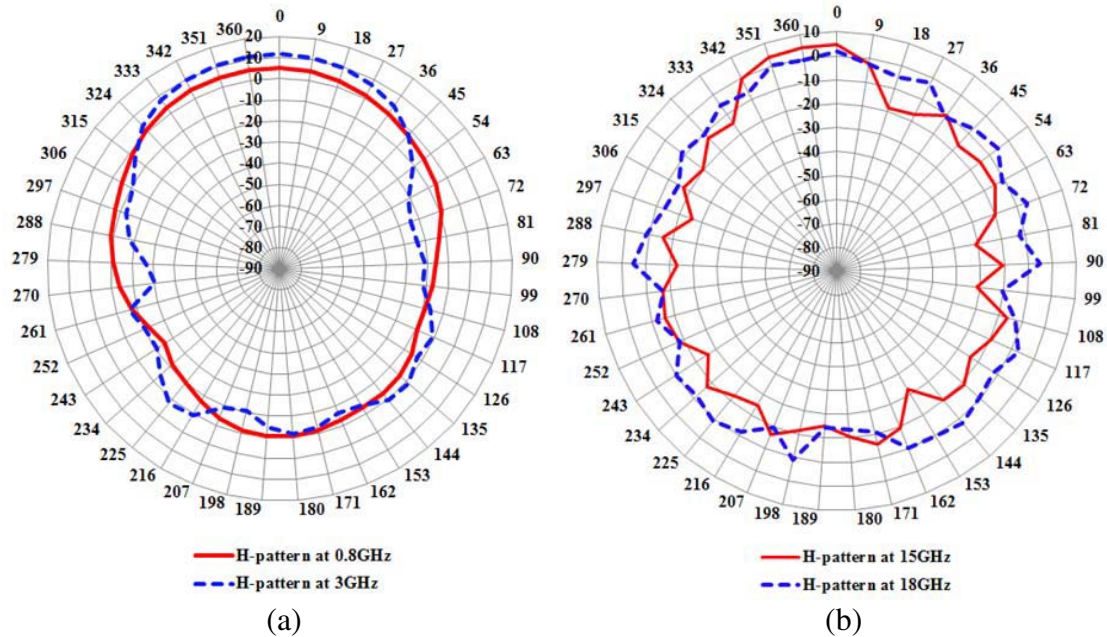
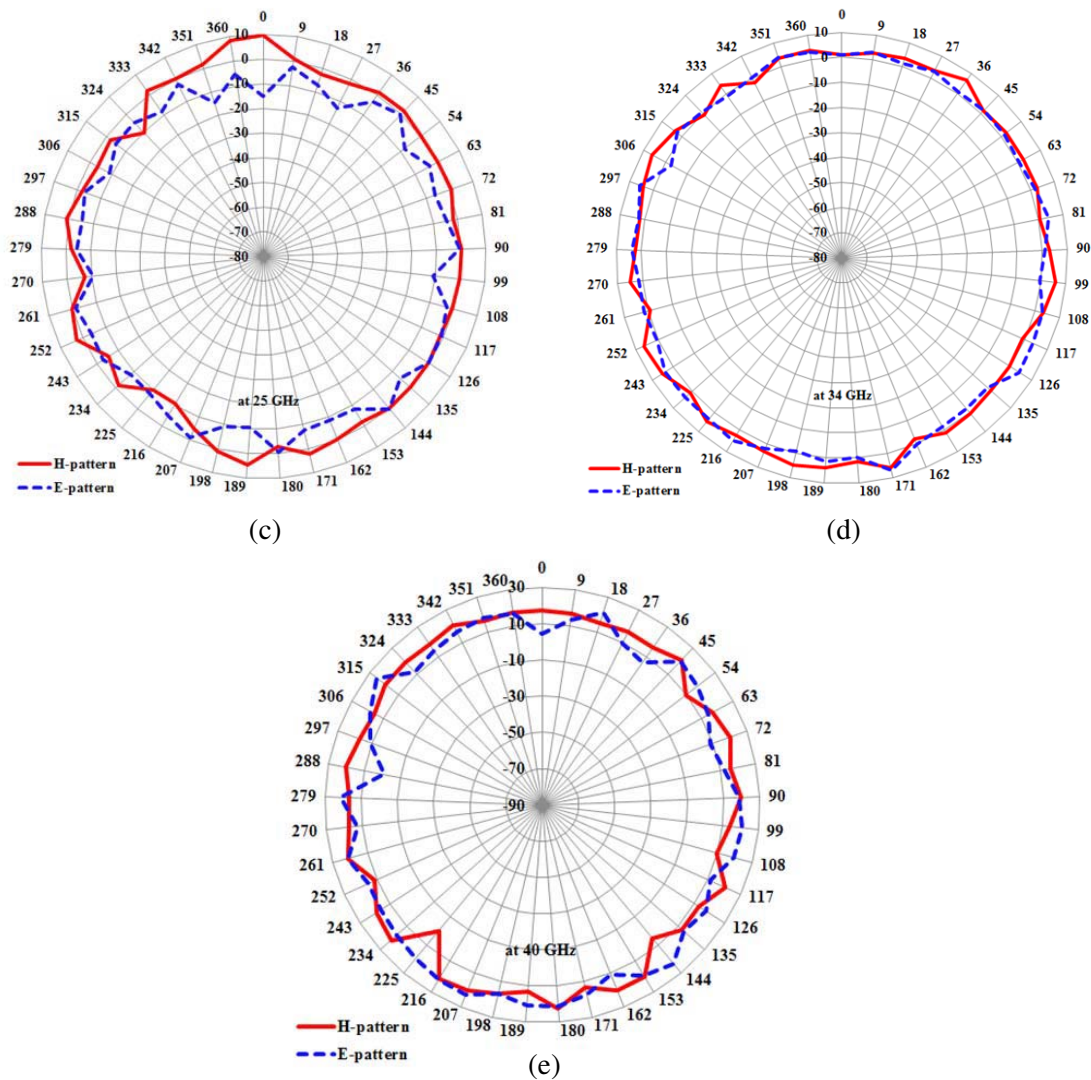


Figure 10. Gain characteristics, (a) RA1, (b) RA2, (c) RA3.





**Figure 11.** Radiation patterns of RA1, RA2 and RA3 at different frequencies measured from newly erected anechoic chamber laboratory *H* plane patterns RA1, (a) 0.8 GHz, 3 GHz, (b) 15 GHz, 18 GHz, RA2 *H* plane & *E* plane patterns, (c) 25 GHz, (d) 34 GHz, (e) 40 GHz.

antennas, respectively; and  $r$  is the distance between transmitter and receiver (in m).

Figure 9 shows the characteristics of  $S_{11}$  (dB) and VSWR of all the RAs whereas their gain characteristics are depicted in Fig. 10. From these characteristics it can be noticed that all the three antennas function as broadband and high gain antennas in the intended frequency ranges.

The *E* and *H* plane radiation characteristics of all these three antennas are depicted in Fig. 11. The solid line indicates the *H* plane, and dotted line shows the *E* plane patterns. It can be noted that the stepper motor used in the control circuitry has a provision to rotate in multiples of  $9^\circ$ ; therefore, the radiation patterns are plotted in steps of  $9^\circ$  instead of the conventionally followed steps of  $10^\circ$ .

#### 4. SUMMARY ON AC SPECIFICATION

The AC, functional in the 0.1 GHz to 40 GHz, has been successfully erected and integrated with VNA and necessary control circuitry. The chamber characterization has been accomplished with overall SE of  $-80$  dB and QZ level of  $-40$  dB. The overall specifications of the AC are summarized in Table 5.

**Table 5.** Chamber specification summary.

| Description                                 | Specification  |
|---|--|
| <b>Chamber Size</b>                         | 7 m × 4 m × 3 m (outer dimensions)                                       |
|   | 6.2 m × 3.3 m × 2.3 m (effective inner dimensions)                       |
| <b>Quiet-Zone Dimension</b>                 | 1 m × 1 m × 1 m (upto 5 GHz)   |
|   | 0.5 m × 0.5 m × 0.5 m (upto 40 GHz)                                      |
| <b>Test Zone Quietness (QZ)</b>             | −40 dB (average level sampled upto 5 GHz, one cubic meter size)          |
| <b>Overall Shielding Effectiveness (SE)</b> | −80 dB (average level sampled at 800 MHz, 5 GHz, 10 GHz, 24 GHz, 40 GHz) |

Some highlights on accessories needed to be fitted inside and outside the AC are listed below:

*Inside the AC:* LED lights inside the chamber, ventilation through air-conditioning unit.

*Outside the AC:* Suitable earthing, CCTV camera and DVR to monitor and record the three-axes motorized system during measurements, power access panel, LCD high resolution monitor, including a fire alarm system, cable access panel on chamber wall, containing adapters 2 N (F to F) and 2 SMA (F to F).

To ensure smooth functionality of AC, to extend the life of established AC facility, and to minimize errors, care should be taken while making use of the AC. The tips of the absorbers should be carefully preserved and should never be touched. To avoid dust, thorough cleaning should only be done using a vacuum cleaner. As prolonged direct exposure to RF radiation is harmful for humans, all measurements should only be carried out by staying outside the chamber.

## 5. CONCLUSION

A rectangular 0.1 GHz to 40 GHz AC of size 7 m × 4 m × 3 m has been proposed, designed, erected, and integrated with VNA, roto-motor system, radiation plotting software, and other necessary accessories. This AC has been validated for SE of −80 dB and QZ of −40 dB. The performance of the setup has been tested for three broadband and high gain horn antennas, and satisfactory performance is provided throughout the frequency range. Even though the chamber has been designed to operate from 0.1 GHz, the practical difficulty of fabricating antennas covering broadband frequencies from 100 MHz to 800 MHz limits the current scope of our work to an operational range from 0.8 GHz to 40 GHz. Hence, the validation of the chamber performance has been carried out accordingly, leaving the validation for lower frequency range as a future scope. This report provides a complete knowledge and intricacies of AC. The described informational guidelines will prove useful to any beginner interested in developing AC. Hence, the established AC is capable of providing a complete test environment for any given antenna.

## ACKNOWLEDGMENT

The authors deeply acknowledge the authorities of CHRIST (Deemed to be University), Bangalore, India for carrying out this research along with establishment of the anechoic chamber and procurement of VNA and SA at the RF and Microwave Research laboratory.

## REFERENCES

1. Hemming, L. H., *Electromagnetic Anechoic Chambers: A Fundamental Design and Specification Guide*, Chapters 1–18, Wiley-IEEE Press, 2002.
2. Emerson, W. H., “Anechoic chamber,” U.S. Patent No. 3,308,463, March 1967.
3. Hemming, L. H., “Anechoic chamber,” U.S. Patent No. 4,507,660, March 1986.

4. Sanchez, G. A., "Geometrically optimized anechoic chamber," U.S. Patent No. 5,631,661, May 1997.
5. Farahbakhsh, A. and M. Khalaj-Amirhosseini, "Metallic spherical anechoic chamber for antenna pattern measurement," *Chin. Phys. B*, Vol. 25, No. 8, 088401, 2016.
6. Farahbakhsh, A. and M. Khalaj-Amirhosseini, "Using metallic ellipsoid anechoic chamber to reduce the absorber usage," *IEEE Transactions on Antennas and Propagation*, Vol. 63, No. 9, 4229–4232, September 2015.
7. Farahbakhsh, A. and D. Zarifi, "Design of metallic parabolic anechoic chamber for compact range measurement," *Electronics Letters*, Vol. 53, No. 5, 294–296, March 2, 2017.
8. Appel-Hansen, J., "Reflectivity level of radio anechoic chambers," *IEEE Transactions on Antennas and Propagation*, Vol. 21, No. 4, 490–498, July 1973.
9. *USAF Handbook for the Design and Construction of HEM P/TEM PEST Shielded Facilities*, AF Regional Civil Engineer Central Region, Dallas, TX, 1987.
10. Hemming, L. H., *Architectural Electromagnetic Shielding Handbook*, IEEE Press, New York, 1992.
11. Morrison, R., *Grounding and Shielding Techniques*, John Wiley & Sons, New York, 1998.
12. Genecco, L. T., *The Design and Shielded Enclosures: Cost Effective Methods to Prevent EMI*, Butterworth-Heinemann, Woburn, MA, 2000.
13. O'Riley, R. P., *Electrical Grounding: Bringing Grounding back to Earth*, 6th edition, Delmar Publishing, Albany, New York, 2001.
14. IEEE Std. 1100-1999, *IEEE Recommended Practice for Powering and Grounding Electronic Equipment*, IEEE Press, New York, 1999.
15. Sanchez, G. and P. Connor, "How much is a dB worth?," *23rd Annual Symposium of the Antenna Measurement Techniques Association (AMTA)*, Denver, Colo., October 2001.
16. Hansen, J. and V. Rodriguez, "Evaluate antenna measurement methods," *Microwave and RF*, October 2010.
17. Rodriguez, V., "Basic rules for anechoic chamber design, Part one: RF absorber approximations," *Microwave Journal*, Vol. 59, No. 1, 72–86, January 2016.
18. IEEE Standard Test Procedures for Antennas, ANSI/IEEE Std 149-1979, 1979.
19. Bennett, J. C. and B. Chambers, "Identification of unwanted scatterers on a free-field EMI test range," *IEEE Proceedings F — Communications, Radar and Signal Processing*, Vol. 130, No. 6, 548–556, October 1983.
20. Thorpe, J. R. and J. C. Bennett, "Characterising the quiet zone of an anechoic chamber," *2004 IEE Antenna Measurements and SAR, AMS 2004*, 2004.
21. "IEEE standard method for measuring the shielding effectiveness of enclosures and boxes having all dimensions between 0.1 m and 2 m," IEEE Std 299.1-2013, 1–96, January 15, 2014.
22. Sheret, T. and B. Allen, "Axis transform to characterise a monopulse twist reflector antenna and radome in an anechoic chamber," *2014 Loughborough Antennas and Propagation Conference (LAPC)*, 612–616, Loughborough, 2014.
23. Rodriguez, V. and E. Barry, "A polynomial approximation for the prediction reflected energy from pyramidal RF absorbers," *Proc. 38th Annu. Symp. Antennas Measurement Techniques Association*, 155–160, October 2016.
24. Xu, Q., Y. Huang, X. Zhu, L. Xing, P. Duxbury, and J. Noonan, "Building a better anechoic chamber: A geometric optics-based systematic solution, simulated and verified [measurements corner]," *IEEE Antennas and Propagation Magazine*, Vol. 58, No. 2, 94–119, April 2016.
25. Chen, Z., Z. Xiong, and A. Enayati, "Limitations of the free space VSWR measurements for chamber validation," *Proc. 38th Annu. Symp. Antenna Measurement Techniques Association*, 144–148, October 2016.
26. Rodriguez, V., "Comparing predicted performance of anechoic chambers to free space VSWR measurements," *2017 Antennas Measurement Techniques Association Symposium (AMTA)*, 1–6, Atlanta, GA, 2017.

27. Xiong, Z., Z. Chen, and J. Chen, "Efficient broadband electromagnetic modeling of anechoic chambers," *2017 11th European Conference on Antennas and Propagation (EUCAP)*, 3747–3750, Paris, 2017.
28. Liao, S., *Microwave Devices and Circuits*, 3rd edition, Prentice Hall, 1990.
29. Raju, G. S. N., *Antennas and Wave Propagation*, 3rd edition, Pearson Education, 2009.
30. Rodriguez, V., "Validation of a method for predicting anechoic chamber performance: A technique that uses polynomial approximations for rf absorber reflectivity," *IEEE Antennas and Propagation Magazine*, Vol. 60, No. 4, 31–40, August 2018.
31. Hunter, E. R. and T. Stander, "A compact, low-cost millimetre-wave anechoic chamber," *2016 10th European Conference on Antennas and Propagation (EuCAP)*, 1–5, Davos, 2016.
32. Chung, B. K., "Anechoic chamber design," *Handbook of Antenna Technologies*, Z. N. Chen, D. Liu, H. Nakano, X. Qing, and Th. Zwick (eds.), Springer, Singapore, 2016.
33. Foged, L. J., M. H. Francis, and V. Rodriguez, "Update of IEEE Std 1720–2012 recommended practice for near-field antenna measurements," *2019 Antenna Measurement Techniques Association Symposium (AMTA)*, 1–3, 2019.
34. Rodriguez, V., *Anechoic Range Design for Electromagnetic Measurements*, Artech House, 2019.
35. Mandaris, D., N. Moonen, S. van de Beek, F. Buesink, and F. Leferink, "Validation of a fully anechoic chamber," *2016 Asia-Pacific International Symposium on Electromagnetic Compatibility (APEMC)*, 865–868, 2016.
36. Tian, B. B., "Free space VSWR method for anechoic chamber electromagnetic performance evaluation," MI Technologies, Technical Papers, 2008.
37. Hao, X., R. Liu, Y. Chen, and J. He, "Calculation and optimization of quiet-zone in RF anechoic chamber," *7th International Symposium on Antennas, Propagation & EM Theory*, IEEE, 2006.
38. IEEE Standards Association Policies and Procedures: <https://standards.ieee.org/standard/299-1969.html>.
39. Military Standard 285: Attenuation Measurements for Enclosures and Electromagnetic Shielding: <https://apps.dtic.mil/dtic/tr/fulltext/u2/771997.pdf>.